Supplementary Information

Dual-functional metasurfaces enabling high-efficiency holography and triple-color printing for enhanced optical security platforms

Harit Keawmuang[1,†], Dohyun Kang[1,†], Xiaotong Li[1,†], Shiqi Hu[1,2], Yeseul Kim[1], Minsu Jeong[1], Chanbeom Jeon[3], Peng Tang[1], Trevon Badloe[4,5,*], and Junsuk Rho[1,3,6,7,]**

[1] Department of Mechanical Engineering, Pohang University of Science and Technology (POSTECH), Pohang 37673, Republic of Korea

[2] Platform for Real-world Innovation in Smart Manufacturing and AI, Korea Advanced Institute of Science and Technology (KAIST), Daejeon 34141, Republic of Korea

[3] Department of Chemical Engineering, Pohang University of Science and Technology (POSTECH), Pohang 37673, Republic of Korea

[4] Department of Electronics and Information Engineering, Korea University, Sejong 30019, Republic of Korea

[5] Division of Smart Energy Convergence Engineering, Korea University, Sejong 30019, Republic of Korea

[6] Department of Electrical Engineering, Pohang University of Science and Technology (POSTECH), Pohang 37673, Republic of Korea

[7] POSCO-POSTECH-RIST Convergence Research Center for Flat Optics and Metaphotonics, Pohang 37673, Republic of Korea

[†]These authors contributed equally to this work.

* trevon@korea.ac.kr

** jsrho@postech.ac.kr

Supplementary Note 1. Simulated conversion efficiency of meta-atoms with varying length and width at the target wavelength

Here, we present parameter sweeps of length (*L*) and width (*W*) for the single (Fig. S1a) and double (Fig. S1b) nanorod configurations. While both cases exhibit regions of high conversion efficiency, we note that the final design geometries are selected by considering not only the efficiency but also the resulting color response.

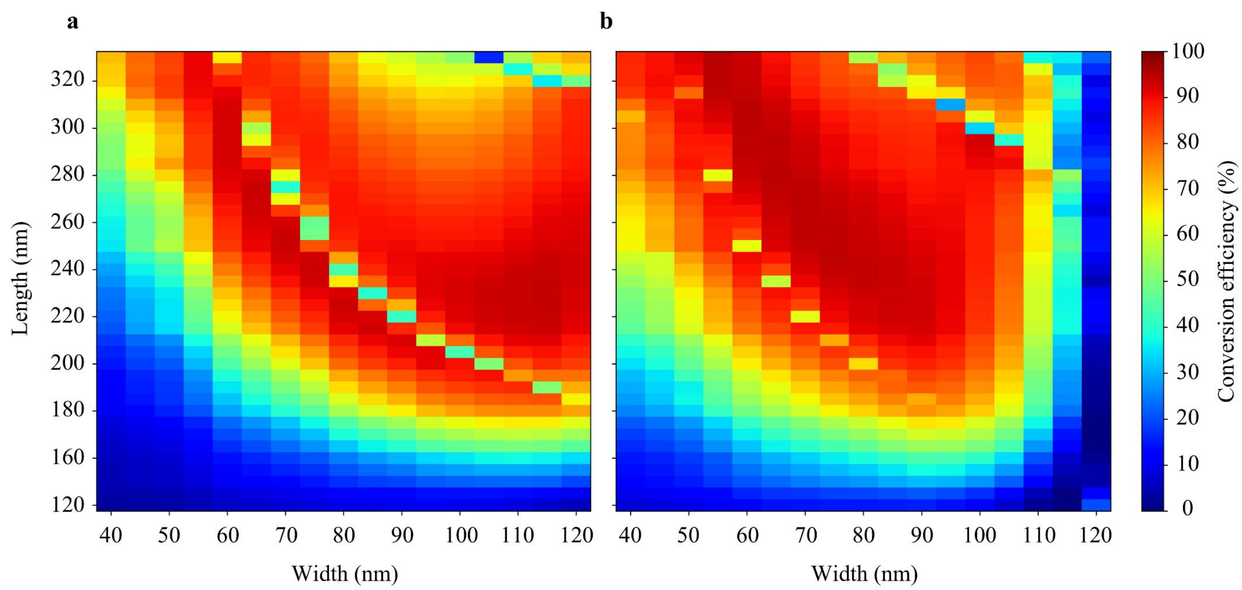

Fig. S1 Simulated conversion efficiency at the target wavelength (640 nm) as a function of meta-atom length L and width W. **a** Single meta-atom configuration. **b** Double meta-atom configuration.

Supplementary Note 2. Effect of gap size on the spectral response and conversion efficiency

Here, we present a parametric study of the gap size in the double nanorod configuration. We simulate reflectance spectra for gaps ranging from 70 to 120 nm and evaluate the corresponding conversion efficiency at the target wavelength of 640 nm. The reflectance spectra show minor variations as the gap changes, while the conversion efficiency remains nearly constant. We note that, in our design, we adopt a gap of 100 nm, consistent with previous literature[1], which also ensures fabrication feasibility and compatibility with our chosen unit cell size.

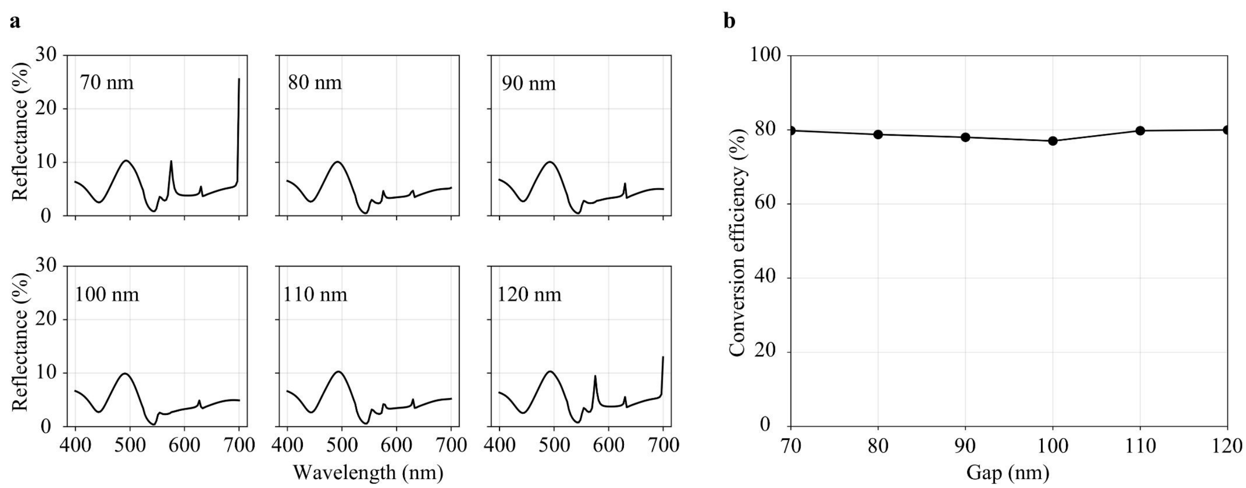

Fig. S2 a Simulated reflectance spectra for different gap sizes (70-120 nm) of double nanorod configuration. **b** Simulated conversion efficiency at 640 nm as a function of gap size.

Supplementary Note 3. Color conversion calculations

Here, we explain the calculation and conversion of the color representation of our metasurface devices. In this study, the CIE 1931 color space system is employed to represent colors derived from the reflectance spectrum using the color matching functions $x(\lambda)$, $y(\lambda)$, and $z(\lambda)$. These functions simulate the observer's chromatic response and are used to compute the tristimulus values X, Y, and Z through the following equations[2]:

$$X = \int_{\lambda_0}^{\lambda_1} R(\lambda) \cdot x(\lambda) \cdot d\lambda \tag{S1}$$

$$Y = \int_{\lambda_0}^{\lambda_1} R(\lambda) \cdot y(\lambda) \cdot d\lambda \tag{S2}$$

$$Z = \int_{\lambda_0}^{\lambda_1} R(\lambda) \cdot z(\lambda) \cdot d\lambda \tag{S3}$$

Here, λ denotes the wavelength of the illumination light with a standard limits λ_0 = 380 and λ_1 = 780 nm, while $R(\lambda)$ corresponds to the reflectance spectrum of the color sample. Although the CIE 1931 standard is defined over 380–780 nm, in this work the integration is effectively limited to 400–700 nm, consistent with the spectral range of reflectance data. Subsequently, the parameters, X, Y, and Z undergo the normalization process to obtain x, y, and z as the chromaticity coordinates:

$$x = \frac{X}{X+Y+Z}, y = \frac{Y}{X+Y+Z}, z = \frac{Z}{X+Y+Z} \tag{S4}$$

To achieve color representation, it is essential to manipulate the chromaticity matrix to transform the tristimulus values from the XYZ color space into RGB (red, green, and blue) color space. This conversion enables the accurate depiction of colors associated with the reflectance spectrum of the sample. Then, the colors representation from the cooler can be realized by using:

$$\begin{bmatrix} R \\ G \\ B \end{bmatrix} = \begin{bmatrix} 0.41847 & -0.15866 & -0.082835 \\ -0.091169 & 0.25243 & 0.015708 \\ 0.0009209 & -0.0025498 & 0.17860 \end{bmatrix} \begin{bmatrix} X \\ Y \\ Z \end{bmatrix} \tag{S5}$$

The transformation from CIE-XYZ to CIE-Lab can be realized by using[3]:

$$L = 116f\left(\frac{Y}{Y_n}\right) - 16 \tag{S6}$$

$$a = 500 \cdot \left(f\left(\frac{X}{X_n}\right) - f\left(\frac{Y}{Y_n}\right)\right) \tag{S7}$$

$$b = 200 \cdot \left(f\left(\frac{X}{X_n}\right) - f\left(\frac{Z}{Z_n}\right)\right) \tag{S8}$$

Where X_n is 95.047, Y_n is 100.00, and Z_n is 108.883 under an illuminant D65. While L represents lightness, a is redness and greenness, and b is yellowness and blueness. Also, the function f can be expressed as

$$f(t) = t^{\frac{1}{3}}, \left(if\ t > \left(\frac{24}{116}\right)^3\right) \tag{S9}$$

$$or\ f(t) = \frac{841}{108} \cdot t + \frac{16}{116}\ if\ otherwise \tag{S10}$$

Supplementary Note 4. Simulated color space for meta-atoms

To design meta-atoms capable of producing distinct structural colors, we simulate and analyze the color space spanned by varying the nanorod dimensions. Fig. S3a presents the color appearance of single- and double-nanorod meta-atoms under white light illumination as a function of length and width. Fig. S3b shows the corresponding chromaticity coordinates mapped onto the CIE 1931 color space. The results confirm that both single (blue squares) and double (red crosses) nanorod designs.

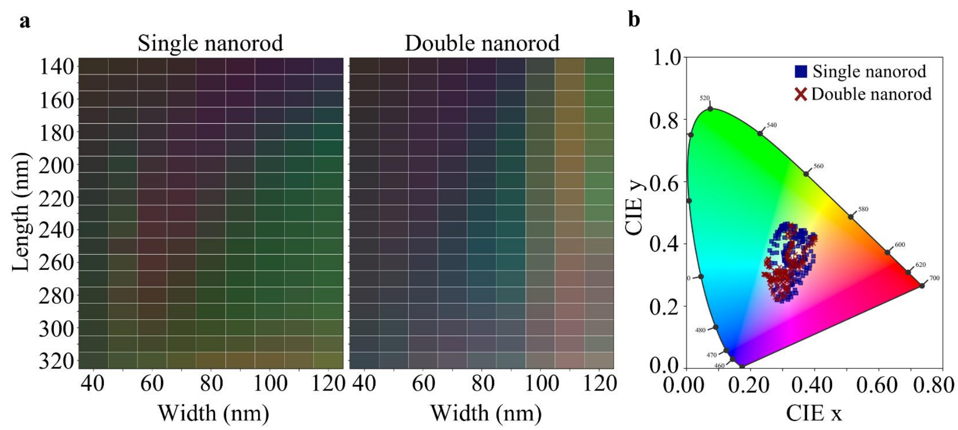

Fig. S3 a Simulated color appearance of single-nanorod and double-nanorod meta-atoms under white light illumination, as a function of nanorod length and width. **b** Corresponding chromaticity coordinates plotted on the CIE 1931 diagram for the single-nanorod (blue squares) and double-nanorod (red crosses) configurations.

Supplementary Note 5. Designed and simulated holographic images

Here, we show the design of Fraunhofer hologram using two different holographic images to be reconstructed in the far-field. We retrieve the holographic images using the Gerchberg-Saxton (GS) algorithm. an iterative method for the phase-only holograms.

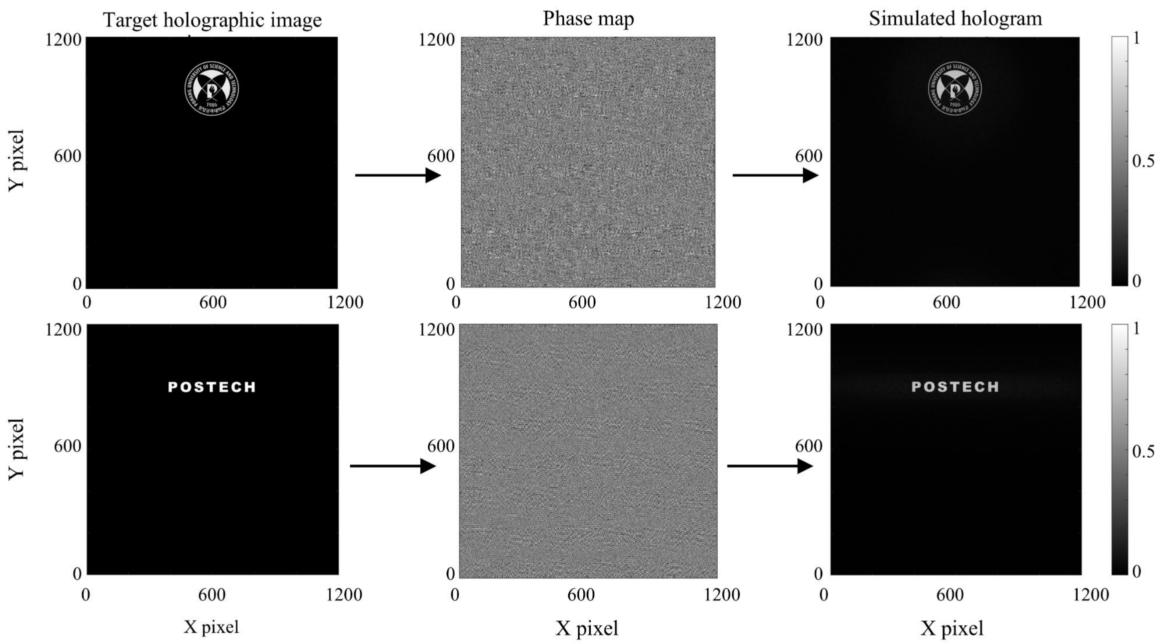

Fig. S4 Designed and simulated holographic images with computer-generated phase map of the hologram.

Supplementary Note 6. Size and off-axis configuration of the holographic images

Here, we compare the target holographic image that match the metasurface pixel with the case where the image size is reduced and an off-axis configuration is applied to avoid the zeroth-order beam (ZOB, represented as the red spot). Fig. S5a shows the original full-size target image, and Fig. S5b schematically illustrates the corresponding reconstructed holographic image. It can be seen that the ZOB severely overlaps with the generated image, degrading fidelity. To address this issue, we revised the target by reducing its size and applying an off-axis configuration, as presented in Fig. S5c. This approach shifts the reconstructed holographic image away from the center, as schematically illustrated in Fig. S5d, thereby avoiding interference from the ZOB.

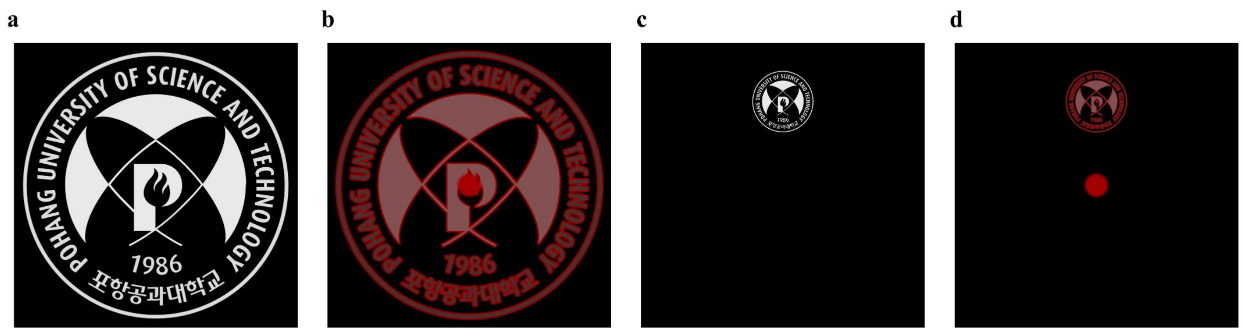

Fig. S5 Schematic illustration of holographic reconstructions with on-axis and off-axis configurations. **a** Original target holographic image. **b** Illustration of the reconstructed holographic image under on-axis configuration without size adjustment, where the zeroth-order beam (ZOB, red spot) overlaps with the desired image. **c** Revised target holographic image with reduced size and off-axis configuration. **d** Illustration of the reconstructed holographic image under off-axis configuration, showing that the ZOB is spatially separated from the desired image, avoiding interference.

Supplementary Note 7. Optical experiment setup for hologram generation

To reconstruct the holographic images, we set up an optical system using a supercontinuum laser as the light source. A tunable bandpass filter is placed at the output to select the desired wavelength. The beam passes through an iris (500 µm) to adjust its size, followed by a linear polarizer (LP) and a quarter-wave plate (QWP) to generate right-handed circularly polarized (RCP). The encoded holographic image is projected on a screen.

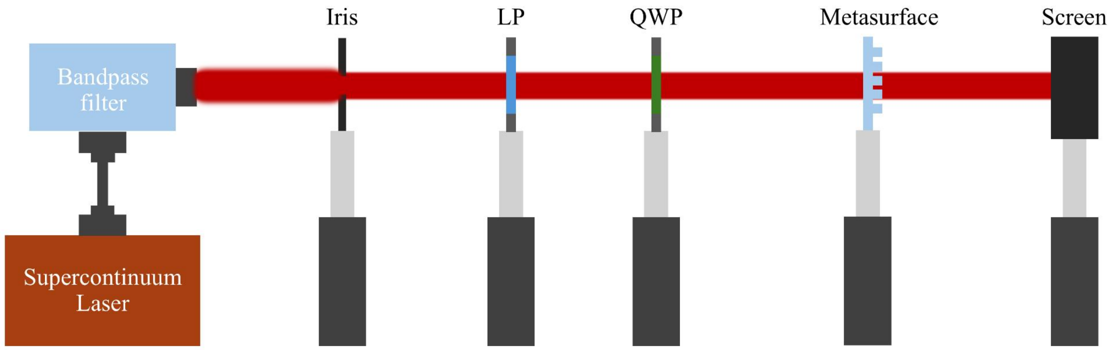

Fig. S6 Schematic illustration of the optical setup used to generate holograms from our dual-functional metasurface.

Supplementary Note 8. Hologram reconstruction under different polarizations

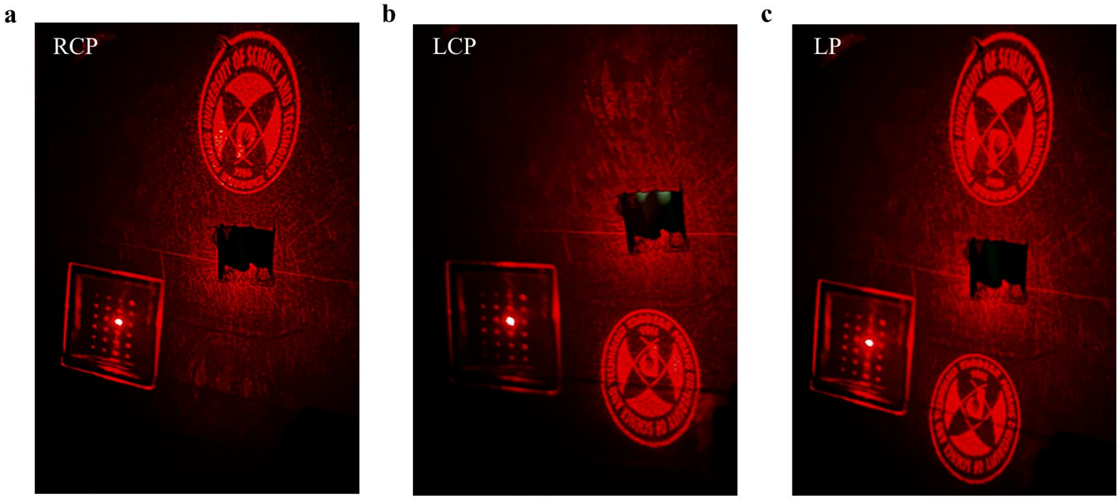

Fig. S7 Reconstructed holographic images from the metasurface under different incident polarization states at a wavelength of 640 nm. **a** Right circularly polarized (RCP) light: the metasurface produces a clear holographic image at the intended position. **b** Left circularly polarized (LCP) light: a centrosymmetric holographic image appears. **c** Linearly polarized (LP) light: both RCP and LCP images appear simultaneously, as LP is a superposition of the two circular polarizations.

Supplementary References

1. Yoon, G. et al. "Crypto-display" in dual-mode metasurfaces by simultaneous control of phase and spectral responses. *ACS Nano* **12**, 6421-6428 (2018).

2. Yoo, Y.J. et al. Ultra-thin films with highly absorbent porous media fine-tunable for coloration and enhanced color purity. *Nanoscale* **9**, 2986-2991 (2017).

3. Fairman, H.S., Brill, M.H. & Hemmendinger, H. How the CIE 1931 color-matching functions were derived from Wright-Guild data. *Color Research & Application* **22**, 11-23 (1997).